Phase mask selection in wavefront coding systems: a design approach

Guillem Carles, Artur Carnicer and Salvador Bosch

Departament de Física Aplicada i Òptica. Universitat de Barcelona. Martí i Franquès 1, E-08028 Barcelona, Spain.

Abstract

A method for optimizing the strength of a parametric phase mask for a wavefront coding imaging system is presented. The method is based on an optimization process that minimizes a proposed merit function. The goal is to achieve modulation transfer function invariance while quantitatively maintaining final image fidelity. A parametric filter that copes with the noise present in the captured images is used to obtain the final images, and this filter is optimized. The whole process results in optimum phase mask strength and optimal parameters for the restoration filter. The results for a particular optical system are presented and tested experimentally in the laboratory. The experimental results show good agreement with the simulations, indicating that the procedure is useful.

Keywords: Imaging Systems, Image Processing, Wavefront Coding, Phase Mask Optimization
PACS: 42.30.Va, 42.30.Lr, 42.30.Wb

1. Introduction

Wavefront coding is based on a combination of digital and optical components in the design of imaging systems. It relies on the optical modification of the transmitted wavefront by means of a phase mask placed at the aperture stop of the system. The design of this phase mask allows image formation that is invariant despite the effects of different optical aberrations[1–4]. Such a modification causes blurring of the images captured by a CCD in the sensor plane. However, these are not the final output of the hybrid system and a postprocessing stage restores the final images. With such a schema,

a hybrid design is able to produce imaging systems with improved depth of field (DOF) which means that the system becomes insensitive to defocus aberration to some extent.

Different aspects need to be considered in the design of the hybrid system. There is a trade-off between the degree of invariance achieved and the final image quality resulting from the strength of the phase mask, the noise power and the restoration filter. All of this is dependent on the specific application particulars.

Moreover, the development of combined optical and digital imaging systems together with the use of programmable spatial light modulators (SLMs) that are able to produce tunable wavefront modification has led to the desirability of flexible wavefront coding imaging systems. This means that a strategy is needed not only to design wavefront coding imaging systems but also to incorporate into these systems the possibility of setting the codification according to the requirements of a specific application.

Apart from a phase mask with a cubic profile[1] and its generalization[5], different alternative shapes have been proposed[6–11]. Also, the literature contains different approaches to optimization of the pupil phase modulation aimed at obtaining defocus insensitivity. Dowski[1] and FitzGerrell[2] suggest an analytical framework based on the use of the Ambiguity Function that allows visualization of the properties of a given one-dimensional wavefront coding design. The requirement that the Ambiguity Function be approximately independent of the defocus leads to the cubic phase mask as the optimum shape among monomial-shaped phase masks. Prasad *et al.*[5] report results for the generalized cubic phase mask, based on other merit criteria. Caron[12] reports an iterative method for optimizing polynomial phase masks (both shape and strength) based on the evaluation of the resultant Modulation Transfer Function (MTF) of the optical system. Other alternatives[13–15] have been reported whose general purpose is to extend the DOF through optimizing the pupil phase modulation, though they are aimed at all-optical imaging systems.

These approaches are all based on evaluation in the intermediate stage, hence they consider only the optical component of the hybrid system. This component is obviously responsible of providing the desired invariance, but limiting evaluation to this stage excludes any effects of the image acquisition and restoration processes. The particular characteristics of them may affect the optimal design of the whole hybrid optical-digital imaging system.

With this in mind, this work proposes a simple and global approach to

evaluating the whole hybrid imaging system, in order to aid the design of wavefront coding imaging systems. The goal is to establish a procedure for the selection of a suitable phase mask strength and the filter parameters, given the characteristics of a particular optical system (optical data, noise power of the sensor, and the invariance required). The procedure concludes defining a selection table that relates the desired invariance range, the optimum phase mask strength and the corresponding associated restoration filter.

The paper is organized as follows. Section 2 relates the basics of wavefront coding theory. The proposed optimization procedure is presented in section 3 and optimization results are summarized in section 4. In section 5 a second optimization procedure for the restoration stage is proposed. Section 6 shows some experimental results that verify the optimizations. Finally, the conclusions are presented in section 7.

2. Theoretical background

Image formation by an optical system under incoherent light illumination can be modeled as the combination of its Point Spread Function (PSF) with the scene imaged (assuming a spatially invariant system). The required operation becomes direct multiplication by the Optical Transfer Function (OTF) in the Fourier space, plus the detection pixelation and noise addition,

$$g = s * h + n \quad \longleftrightarrow \quad G = S \cdot H + N \tag{1}$$

where g is the captured image, h is the PSF of the system, s is the pixelated scene that is imaged and n is the noise realization present in the captured image; the capital letters correspond to the discrete Fourier transforms.

For an aberration-free optical system, the presence of a phase mask modifies the pupil wavefront from the diffraction limited field, changing the OTF of the system. For a defocused wavefront coding system, H is,

$$H(W_{20}, \phi) = R\Big[e^{i\cdot 2\pi\cdot W_{20}(x^2+y^2)} \cdot e^{i\cdot 2\pi\cdot \phi(x,y)} \cdot P(x,y)\Big] \tag{2}$$

where R stands for the autocorrelation operator, W_{20} is the defocus aberration parameter, (x, y) are the pupil coordinates normalized at the pupil aperture, ϕ is the modulation introduced by the phase mask and P is the limitation of the aperture pupil of the system, i.e.,

$$P(x,y) = \begin{cases} 1 & \text{if } (x,y) \text{ is inside the aperture} \\ 0 & \text{if } (x,y) \text{ is outside the aperture} \end{cases}, \tag{3}$$

The modulation introduced by a cubic phase mask is expressed as,

$$\phi_c(x,y) = \alpha\left(x^3 + y^3\right) \tag{4}$$

where α determines the strength of the phase mask. Another commonly used mask is the generalized cubic phase mask,

$$\phi_g(x,y) = \alpha\left(x^3 + y^3\right) + \beta\left(x^2 y + y^2 x\right) \tag{5}$$

where $\beta = -3\alpha$ is usually assumed[5].

The restored scene will be,

$$r = \mathcal{F}^{-1}\Big\{G \cdot F \cdot H_{dl}\Big\} \tag{6}$$

where $\mathcal{F}^{-1}$ stands for inverse Fourier transformation, F is the restoration filter defined in the Fourier space and H_{dl} is the OTF of the system limited by diffraction; i.e.,

$$H_{dl} = R\big[P(x,y)\big]. \tag{7}$$

H_{dl} is incorporated in Eq. 6 because the restoration process only aims to recover the optical modification produced by the phase mask. One very basic choice for F is the Wiener filter[16],

$$F = \frac{H_c^*}{H_c^2 + K} \tag{8}$$

where * denotes a complex conjugate, H_c is the OTF restoration-kernel (typically the OTF of the system with aberration centered on the invariance range),

$$H_c(\phi) = R\big[e^{i\cdot 2\pi\cdot\phi(x,y)} \cdot P(x,y)\big], \tag{9}$$

and K is the ratio between the noise and the scene power spectra. When the noise and scene power spectra are not known, an adjustable constant k and a frequency-function dependency are considered; namely,

$$K = k\left(u^2 + v^2\right)^{\omega} \tag{10}$$

where (u, v) are the frequencies in the Fourier plane. When $\omega = 0$, F becomes the parametric Wiener filter. Eq. 10 corresponds to a white noise assumption and a frequency dependency given by the type of scenes to be restored [17,18].

Since defocus aberration is symmetric with respect to the infocus plane, the invariance range will be $[-W_{20}, W_{20}]$, which corresponds to the extended DOF of the imaging system. Thus, the aberration-free OTF of the system will be used in Eq. 8 as the restoration-kernel OTF.

An important drawback of wavefront coding techniques is noise amplification in the images. Since the effect of the phase mask is to broaden the PSF, and hence to reduce the MTF, the noise present in the captured images will undergo the same restoration process and be unavoidably amplified [19].

3. Phase mask strength optimization

Regardless of the shape of its phase mask, a wavefront coding imaging system is expected to reduce image quality but to increase aberration invariance as the strength of the phase mask increases. Thus, as mentioned above, the goal of this work is to obtain the phase mask strength that best suits the trade-off between invariance to defocus and image fidelity. The procedure consists of obtaining the solution by minimizing a given merit function. The merit function proposed is,

$$\Psi(W_{20}, \phi) = \mathrm{RMS}\Big\{ \big|T\left(W_{20}, \phi\right)\big| - \big|H_{dl}\big| \Big\} \tag{11}$$

where $\mathrm{RMS}\{\cdot\}$ stands for the root mean squared operator and T is the restored OTF of the imaging system. Using Eqs. 2 and 8,

$$T(W_{20}, \phi) = H(W_{20}, \phi) \frac{H_c^*(\phi) H_{dl}}{|H_c(\phi)|^2 + K} \tag{12}$$

Note the explicit dependency of T on the defocus aberration and on the phase mask profile.

Different remarks can be made concerning the definition in Eq. 11. Firstly, it is implicitly assumed that the intermediate levels of degradation (any amount below that specified by the desired invariance) will also produce an intermediate quality image. This fact is not strictly true, as it is possible that $\Psi(W'_{20}, \phi) > \Psi(W_{20}, \phi)$ for $W'_{20} < W_{20}$. But in practice, as the phase mask shape is fixed, this is small enough to be neglected, as illustrated in section 4. Secondly, the merit function directly accounts for both the invariance

achieved and the image fidelity since they are compared for the diffraction limited OTF, H_{dl}, instead of the restored OTF with no aberration, $T(0, \phi)$. This penalizes excess codification. Thirdly, the comparison is made once the detection and restoration stages have been performed, and hence accounts for any influence they may have. And finally, it is worth mentioning that since it is based on OTF analysis, it leads to a general design and does not require any particular scene to evaluate the imaging performance (which would influence the evaluation and be vulnerable to PSF shifting or mismatching effects[4]).

Furthermore, note that no noise considerations are taken into account in this merit measure. This is deliberate, since it is assumed that the best noise filtering strategy is inherently incorporated in the restoration filter. Clarifying how this may affect the results is the goal of section 5.

4. Optimization results

Without any lose of generality, the pupil phase modulation of a phase mask can be expressed as,

$$\phi(x, y) = \gamma \cdot \varphi(x, y) \tag{13}$$

where ϕ is the actual modulation surface in the pupil area, φ the same surface with a peak-to-valley modulation of one wavelength across the whole pupil area and γ is a scale factor relating the two. The value (in terms of wavelengths) of γ will be called the strength of the phase mask. For the case of cubic or generalized cubic phase masks, γ is proportional to α, with the constant of proportionality depending on the pupil shape. Using this approach, it is feasible to compare different phase masks or even phase masks with different pupil shapes, as the γ value represents the strength of the codification imposed.

The simulations presented here correspond to modeling of an imaging system with a rectangular pupil. The coordinate normalization is carried out at the corner distance; if (x_{pup}, y_{pup}) are the rectangular pupil coordinates,

$$\begin{cases} x &= 2 \cdot x_{pup}/L \\ y &= 2 \cdot y_{pup}/L \\ L &= \sqrt{L_x^2 + L_y^2} \end{cases} \tag{14}$$

The dependency of the proposed merit function on the defocus aberration and on the phase mask strength for the cases of cubic and generalized cubic phase masks is presented in Fig. 1 (a) and (b). A parametric Wiener filter with $k = 0.01$ was used in the calculations (k near this value turns to be adequate for a common scene and a common 8-bits-depth CCD camera, see section 5). Fig. 1(c) shows different profiles of constant γ for the cubic mask. The invariance is reflected as a constant merit value, while the value itself gives an idea of the imaging fidelity. In Fig. 1(d) different profiles of constant W_{20} are shown. It can be seen that Ψ penalizes both a lack and an excess of codification, thus reflecting the physical trade-off between providing sufficient invariance without resulting in too great a loss of imaging fidelity. Thus, the minima in Fig. 1(d) represent the optimum phase mask strength resulting from the proposed merit function for a desired invariance range.

Fig. 1(d) illustrates the cases of setting the desired range of invariance to $W_{20} = 5\lambda$ and $W_{20} = 10\lambda$. Plotting the position of the minimum as a function of the desired amount of invariance, W_{20}, gives the results shown in Fig. 2. The relationship shown in this figure can be interpreted as the selection table that relates the amount of codification (the optimum phase mask strength) given the desired invariance range. As can be seen, the plot exhibits a linear trend regardless of the shape of the phase mask. This is in accordance with the theoretical predictions made by Muyo [20] and Pan [21] for the cubic phase mask. Here the results are obtained for a rectangular pupil shape with the detection and restoration stages accounted for. The behavior of the merit function with respect to the phase mask strength reveals a double local minima for the case of the cubic phase mask, see Fig. 1(d). The first minimum is the global for $W_{20} < 10.3\lambda$ and the second becomes the global above that value; this threshold depends on the k value and the desired invariance. This change in the global minimum leads to the step seen in Fig. 2. This phenomenon is not present for the generalized cubic phase mask.

5. Restoration

The diffraction limited properties must be restored from the image formed and also the noise present in the captured image must be filtered, i.e., the contributions of those frequencies which exhibit lower signal-to-noise ratio values must be reduced. Thus a higher noise power will result in more severe image filtering and hence in a lose of final imaging quality. Since this

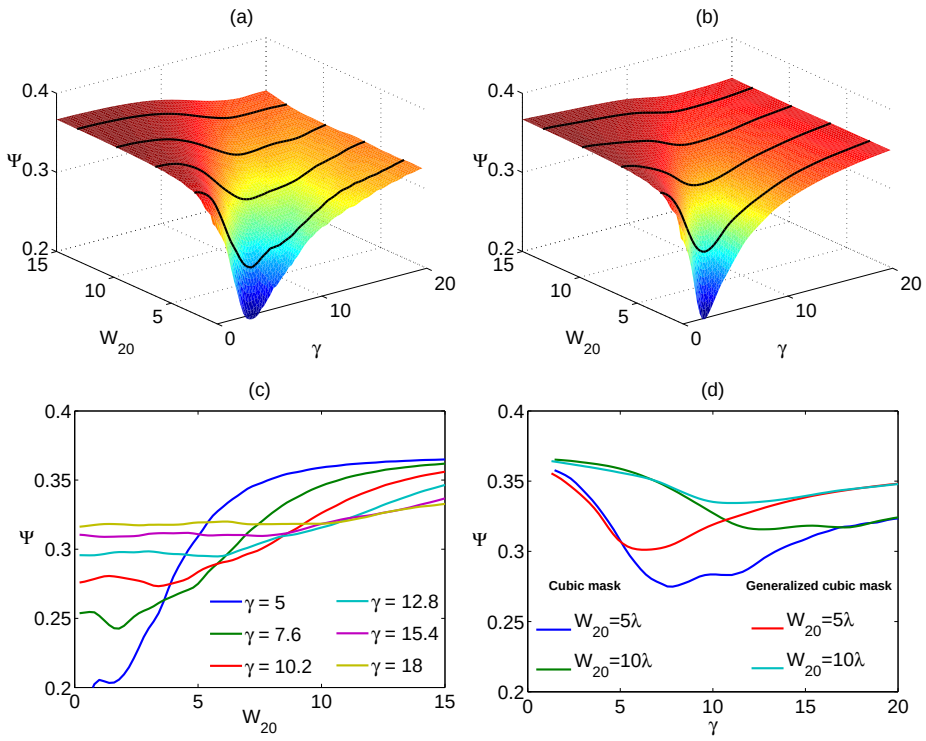

Figure 1: Dependency of the merit function on the defocus aberration and the parameter γ of (a) a cubic phase mask and (b) a generalized cubic phase mask (with $\beta = -3\alpha$), using a parametric Wiener filter with $k = 0.01$ (related to image intensities in the range $[0, 1]$). (c) Profiles of constant γ, for different values of γ and for the cubic phase mask. (d) Profiles of constant W_{20}, for different values of W_{20} and phase mask shapes.

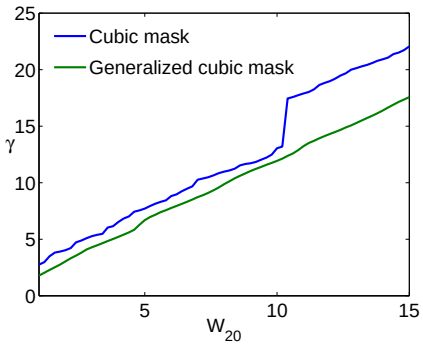

Figure 2: Phase mask strength optimization results as a function of the desired invariance.

Figure 3: Image used to evaluate the quality of the restored scene.

will affect the final performance of the hybrid imaging system, it must be accounted for.

To take into account the effects of noise on the spectral distribution, a particular image has to be considered. Here, the scene shown in Fig. 3 is used. In addition, an appropriate metric to assess the similarity between the original scene and the restoration is needed. This is a subjective visual perception-based evaluation and measures such as the pixel-wise RMS difference are not appropriate. In this work, the structural similarity index (SSIM) is used[22]. This index is an image quality metric that accounts for the structural information variation in the image, resulting in a figure of merit for image similarity closer to human visual perception. The SSIM is bounded between 0 and 1, with 1 being maximum similarity. For convenience, the evaluation will be carried out using the dissimilarity measure M defined as,

$$M = 1 - \mathrm{MSSIM}\Big[r(W_{20} = 0, k); s_{dl}\Big] \tag{15}$$

where MSSIM is the mean similarity index with its default settings as defined in[22], and s_{dl} is the scene imaged with the conventional system (without a phase mask), i.e., limited by diffraction.

The minimization of Eq. 15 leads to the best value of k for the filter. Using the parametric Wiener filter the behavior shown in Fig. 4 holds. It is interesting to note that the minimum differs depending on the phase mask strength. Using this procedure to find the restoration filter is an advantage because the best value in terms of Eq. 15 is extracted regardless of the actual noise and scene power spectra ratio, or any possible phase mask influence.

Finally, for the sake of completeness, it is worth noting that the results of

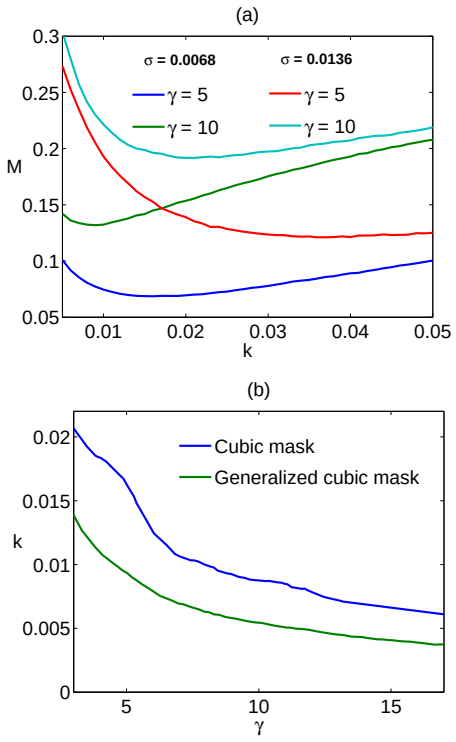

Figure 4: (a) M as a function of k for different phase mask strengths and different values of the added noise power; using the cubic phase mask and the parametric Wiener filter. (b) Optimum k value as a function of the phase mask strength, for $\sigma_{noise} = 0.0068$. The values for σ_{noise} and k are related to image intensities in the range $[0, 1]$.

Table 1: Optimization results for the cubic phase mask, for different required DOFs.

DOF (W_{20})	γ	α	k
1λ	2.8λ	1.9λ	0.02199
2λ	4.0λ	2.8λ	0.01834
3λ	5.3λ	3.6λ	0.01536
4λ	6.5λ	4.5λ	0.01152
5λ	7.7λ	5.3λ	0.01024
6λ	8.8λ	6.1λ	0.00930
7λ	10.3λ	7.1λ	0.00871
8λ	11.0λ	7.6λ	0.00849
9λ	11.7λ	8.1λ	0.00813
10λ	13.0λ	9.0λ	0.00718
11λ	17.9λ	12.3λ	0.00591
12λ	19.0λ	13.1λ	0.00565
13λ	20.1λ	13.9λ	0.00541
14λ	20.9λ	14.4λ	0.00519
15λ	22.1λ	15.2λ	0.00496

this section do not substantially change the phase mask strength optimization results (at least, not for the phase mask shapes tested), hence no coupling is found between the two optimization processes.

6. Experimental verification

Combining the results of sections 4 and 5 the optimum strengths and k values as a function of the required DOF can be summarized as a selection table. Table 1 shows the results for the cubic phase mask and table 2 for the generalized cubic phase mask.

To verify the results, a wavefront coding imaging system was implemented in the laboratory. Fig. 5 shows the layout and Table 3 the specifications. The optical system is composed of a simple lens. A CCD camera is placed at a fixed distance (also fixing the position of the paraxial object plane). To produce the phase modulation at the pupil, an SLM and two polarizers are introduced [23,24]. In this system, the element limiting the pupil is the SLM itself, which has a rectangular shape.

Fig. 6 shows the experimental results using the resolution USAF target. Effectively, the resolved frequencies for each case show the values $\gamma = 7.7$ and $\gamma = 13.0$ as good compromises between defocus removal and lose of imaging

Table 2: Optimization results for the generalized cubic phase mask, for different required DOFs.

DOF (W_{20})	γ	α	k
1λ	1.8λ	0.7λ	0.02267
2λ	3.0λ	1.2λ	0.01370
3λ	4.3λ	1.7λ	0.01044
4λ	5.2λ	2.0λ	0.00900
5λ	6.7λ	2.6λ	0.00720
6λ	7.8λ	3.0λ	0.00646
7λ	8.7λ	3.4λ	0.00590
8λ	9.9λ	3.8λ	0.00546
9λ	11.0λ	4.3λ	0.00507
10λ	11.9λ	4.6λ	0.00487
11λ	13.2λ	5.2λ	0.00447
12λ	14.3λ	5.6λ	0.00419
13λ	15.3λ	6.0λ	0.00401
14λ	16.4λ	6.4λ	0.00379
15λ	17.6λ	6.8λ	0.00366

Table 3: Optical system specifications, related to schema in Fig. 5. The standard deviation noise parameter is related to image intensities in the range $[0, 1]$.

Parameter	Value
SLM cell pitch	42 μm
CCD pixel pitch	4.65 μm
Lens focal length	206 mm
L_x	26.9 mm
L_y	20.2 mm
d	315.1 mm
σ_{noise}	0.0068
Working wavelength	633 nm

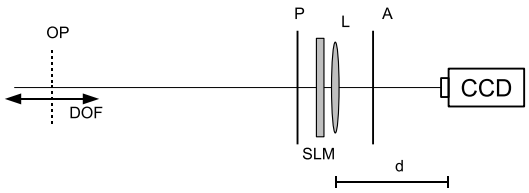

Figure 5: Optical system setup in the laboratory. OP: Object Plane; DOF: Depth Of Field; P: Polarizer; A: Analyzer; SLM: Spatial Light Modulator; L: Lens. CCD: Camera; d: fixed distance.

quality, for the cases of $W_{20} = 5\lambda$ and $W_{20} = 10\lambda$ respectively. Fig. 7 shows the homologous results using a typical scene. Again, although artifacts are present in the images due to PSF mismatching, the restored scenes confirm the same values that balance the discussed trade-off well.

In summary, both figures show that too low a phase mask strength does not provide enough invariance, whereas too high a phase mask strength degrades the image unnecessarily and leads to a lose of imaging fidelity. Intermediate values encountered in the optimization procedure show reasonably good performance across the whole design invariance range.

7. Conclusions

A procedure for selecting the strength of a phase mask for wavefront coding imaging systems has been presented. This procedure allows selection of both the phase mask strength and the parameters of the restoration filter of a wavefront coding imaging system.

Two subprocesses are used. An optimization process finds the most suitable phase mask strength by minimizing a merit function based on the restored and aberration-degraded OTF, given a required DOF. This process accounts for the trade-off between invariance achieved and imaging fidelity. A second optimization process identifies the parameters of the filter that minimize a merit function based on a particular scene; this process determines optimal filter design and accounts for both the noise in the image acquisition process and its effect on the restoration process.

The procedure was applied to a particular optical system and the solutions obtained were tested experimentally in the laboratory. The results show good agreement with the simulations, indicating that the procedure is indeed valid.

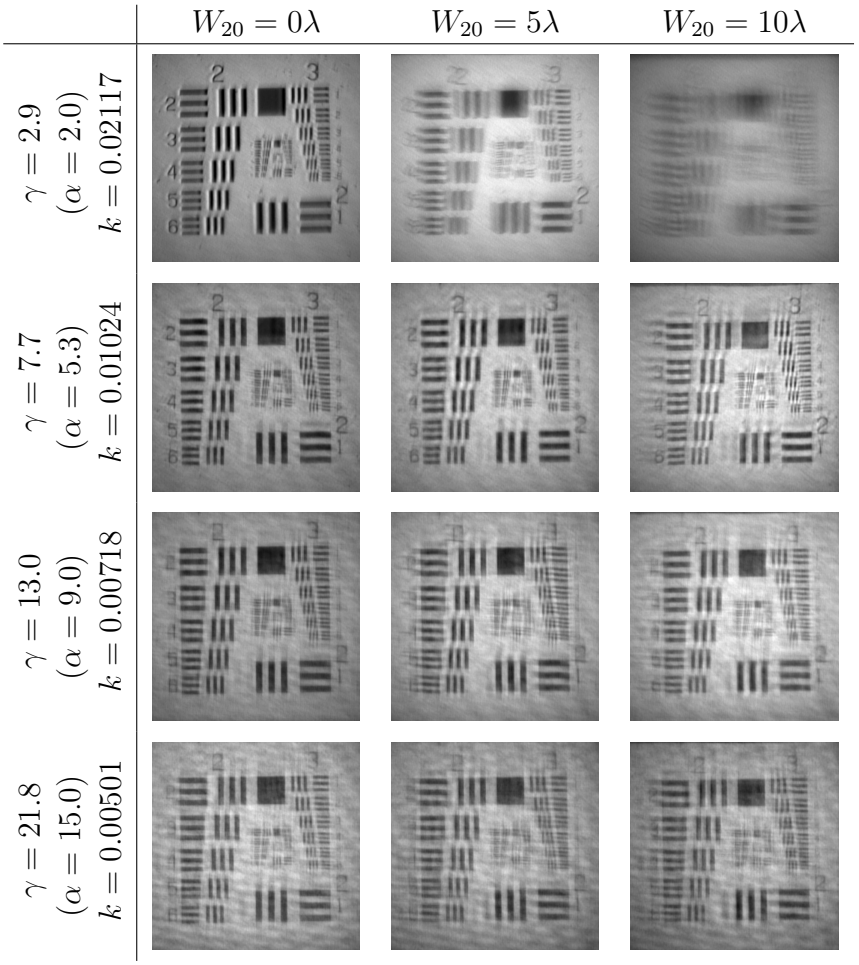

Figure 6: Restored scenes of the USAF resolution target using different cubic phase mask strengths and different amounts of defocus aberration, obtained experimentally in the laboratory. The values of the parameter k of the filter are related to image intensities in the range $[0, 1]$.

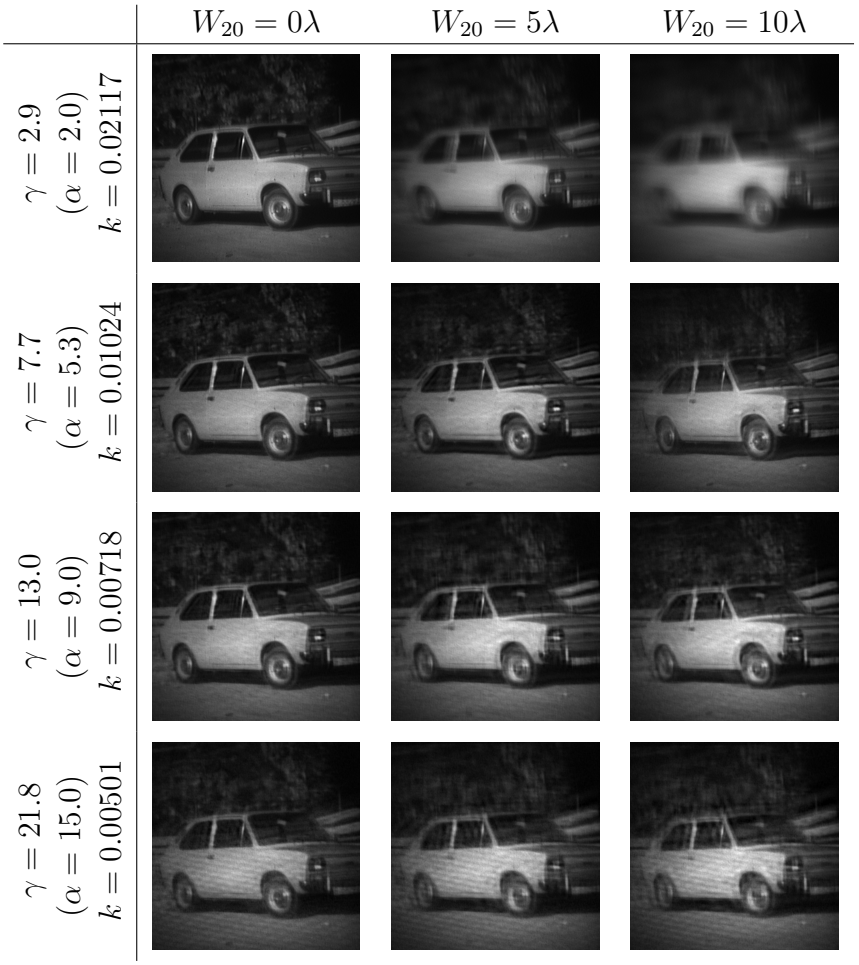

Figure 7: Restored scenes of a particular landscape using different cubic phase mask strengths and different amounts of defocus aberration, obtained experimentally in the laboratory. The values of the parameter k of the filter are related to image intensities in the range $[0, 1]$.

Acknowledgments

The authors would like to thank Dr. Santiago Vallmitjana and Ms. Carme Ferran for their helpful comments and suggestions. This paper has been supported in part by the CICYT (the Spanish R&D Agency) project DPI2008-04175. Guillem Carles gratefully acknowledges the financial support of FPI grant BES-2006-12357 from the Spanish Ministry of Science and Innovation.

[1] J. Edward R. Dowski, W. T. Cathey, Extended depth of field through wave-front coding, APPLIED OPTICS 34 (11) (1995) 1859–1866.

[2] A. FitzGerrell, E. Dowski, W. Cathey, Defocus transfer function for circularly symmetric pupils, APPLIED OPTICS 36 (23) (1997) 5796–5804.

[3] W. Cathey, E. Dowski, New paradigm for imaging systems, APPLIED OPTICS 41 (29) (2002) 6080–6092.

[4] W. Zhang, Z. Ye, T. Zhao, Y. Chen, F. Yu, Point spread function characteristics analysis of the wavefront coding system, OPTICS EXPRESS 15 (4) (2007) 1543–1552.

[5] S. Prasad, T. Torgersen, V. Pauca, R. Plemmons, J. van der Gracht, High-resolution imaging using integrated optical systems, INTERNATIONAL JOURNAL OF IMAGING SYSTEMS AND TECHNOLOGY 14 (2) (2004) 67–74.

[6] S. Sherif, W. Cathey, E. Dowski, Phase plate to extend the depth of field of incoherent hybrid imaging systems, APPLIED OPTICS 43 (13) (2004) 2709–2721.

[7] Q. Yang, L. Liu, H. Sun, Optimized phase pupil masks for extended depths of field, OPTICS COMMUNICATIONS 272 (1) (2007) 56–66.

[8] K. Kubala, E. Dowski, W. Cathey, Reducing complexity in computational imaging systems, Opt. Express 11 (18) (2003) 2102–2108.

[9] A. Castro, J. Ojeda-Castaneda, Asymmetric phase masks for extended depth of field, APPLIED OPTICS 43 (17) (2004) 3474–3479.

[10] S. Mezouari, A. Harvey, Phase pupil functions for reduction of defocus and spherical aberrations, OPTICS LETTERS 28 (10) (2003) 771–773.

[11] A. Sauceda, J. Ojeda-Castaneda, High focal depth with fractional-power wave fronts, OPTICS LETTERS 29 (6) (2004) 560–562.

[12] N. Caron, Y. Sheng, Polynomial phase masks for extending the depth of field of a microscope, APPLIED OPTICS 47 (22) (2008) E39–E43.

[13] E. Ben-Eliezer, E. Marom, N. Konforti, Z. Zalevsky, Radial mask for imaging systems that exhibit high resolution and extended depths of field, APPLIED OPTICS 45 (9) (2006) 2001–2013.

[14] D. Zalvidea, C. Colautti, E. Sicre, Quality parameters analysis of optical imaging systems with enhanced focal depth using the Wigner distribution function, JOURNAL OF THE OPTICAL SOCIETY OF AMERICA A-OPTICS IMAGE SCIENCE AND VISION 17 (5) (2000) 867–873.

[15] D. Zalvidea, E. Sicre, Phase pupil functions for focal-depth enhancement derived from a Wigner distribution function, APPLIED OPTICS 37 (17) (1998) 3623–3627.

[16] R. C. Gonzalez, R. E. Woods, Digital Image Processing, Addison-Wesley Longman Publishing Co., Inc., Boston, MA, USA, 1992.

[17] G. J. Burton, I. R. Moorhead, Color and spatial structure in natural scenes, APPLIED OPTICS 26 (1) (1987) 157–170.

[18] D. J. Field, Relations between the statistics of natural images and the response properties of cortical cells, JOURNAL OF THE OPTICAL SOCIETY OF AMERICA A-OPTICS IMAGE SCIENCE AND VISION 4 (12) (1987) 2379–2394.

[19] S. Sherif, E. Dowski, W. Cathey, Effect of detector noise in incoherent hybrid imaging systems, OPTICS LETTERS 30 (19) (2005) 2566–2568.

[20] G. Muyo, A. Harvey, Decomposition of the optical transfer function: wavefront coding imaging systems, OPTICS LETTERS 30 (20) (2005) 2715–2717.

[21] C. Pan, J. Chen, R. Zhang, S. Zhuang, Extension ratio of depth of field by wavefront coding method, OPTICS EXPRESS 16 (17) (2008) 13364–13371.

[22] Z. Wang, A. Bovik, H. Sheikh, E. Simoncelli, Image quality assessment: from error visibility to structural similarity, IMAGE PROCESSING, IEEE TRANSACTIONS ON 13 (4) (2004) 600–612.

[23] G. Carles, G. Muyo, S. Bosch, A. R. Harvey, Implementation of a wavefront coded imaging system using a spatial light modulator, Vol. 7100, SPIE, 2008, p. 71000X.

[24] D. Hong, K. Park, H. Cho, M. Kim, Flexible depth-of-field imaging system using a spatial light modulator, APPLIED OPTICS 46 (36) (2007) 8591–8599.